

Total-energy-based structure prediction for d(AlNiCo)

C.L. Henley¹, M. Mihalkovič^{2,3}, and M. Widom⁴

¹ Department of Physics, Cornell University, Ithaca NY 14853

² Institute für Physik, Technische Universität Chemnitz, D-09107 Germany

³ Institute of Physics, Slovak Academy of Sciences, Bratislava, Slovakia

⁴ Department of Physics, Carnegie-Mellon University, Pittsburgh PA 15213

(October 25, 2018)

One may predict a quasicrystal structure starting from electrons and quantum mechanics, as approximated by interatomic pair potentials calibrated with ab-initio total-energy calculations, combined with the experimentally known composition and lattice constants. Here we report our progress on the “basic Ni” decagonal phase $d(\text{Al}_{70}\text{Ni}_{21}\text{Co}_9)$. Atomic configurations are represented as decorations of (possibly) random tilings. Our method was Monte Carlo simulation using both lattice-gas hops by atoms and tile-flip rearrangements, eventually followed by molecular dynamics and relaxation of the atom positions. Initially allowing the greatest freedom of atom positions, we observed nearly deterministic structural rules and enforced these as constraints involving larger tiles; this procedure was repeated at the next level of modeling. In crude and preliminary form, the effective Hamiltonian for tile-tile interactions is known, which is needed for further simulations to infer the long-range order. Our atomic arrangements in the 20 Å decagonal cluster are compared with three structure models based on recent experiments.¹

I. INTRODUCTION

This paper reports on early results of a program to determine the structure of a quasicrystal – specifically $d(\text{AlNiCo})$ – strictly from energetics, without use of diffraction data. Almost all of the work was performed by M.M. and M.W., with their coauthors, and is reported in Ref. [1], but the present account is tilted towards the particular interests of C.L.H.

We have focused on the thermodynamically stable and highly ordered “Basic Nickel” subphase of decagonal $d(\text{AlNiCo})$ [2,3], of composition approximately $\text{Al}_{0.70}\text{Ni}_{0.21}\text{Co}_{0.09}$. Our ultimate objective is to *predict* the structure on the basis of total energy; though the gross aspects of the structure are clear from diffraction, there are many ambiguous or controversial details, and there is no understanding for the quasicrystal’s special stability and simplicity at this composition. In particular, we wish to identify the sites of the transition metal

(“TM”) components Ni and Co, which are indistinguishable to (ordinary) X-rays or electrons [4–8].

In a sense, the most difficult problem of crystal chemistry is to predict which structure a given composition will adopt, even if one has an exact and tractable Hamiltonian for the total energy (e.g. by pair potentials) – for this necessarily involves a comparison with an *infinity* of possible structures. The only irreproachable method is a mathematical proof, which is feasible in rare cases with short-range interactions, e.g. close-packing of hard spheres, or the two-dimensional “binary-tiling” quasicrystal (a toy model) [9]. A naive, brute-force approach would be to cool (in simulation) from the melt, and see which structures emerge; but this is prone to fail for a complicated material, since the accessible times are so short that it will get stuck in a glassy disordered configuration. Even when a quasicrystal emerges, as with Dzugutov’s toy potentials [10], the system may have found a merely metastable ordered state for kinetic reasons: indeed, the stable phase in this case turned out to be a simple bcc packing [11].

II. DECORATION MODELS

We represent the quasicrystal structure as a decoration of *disjoint* tiles. There are several reasons for doing so, rather than as a irrational cut through a five-dimensional hypercrystal. Based in real space, this representation is easier to visualize and somewhat more tractable, technically, than the hypercrystal approach. For example, shifts of the atoms from ideal (tiling-vertex) sites are parametrized by just a finite set of real numbers, like the coordinates in a crystal unit cell. A decoration description – particularly in the decagonal case – naturally lends itself to a hierarchy of supertilings, which are presumably involved in the modulations which distinguish some of the subphases in the $d(\text{AlNiCo})$ phase diagram [3]. Furthermore, most hyperspace structures which have been defined using discrete acceptance domains, e.g. Ref. [4], can be translated into tiling-decoration language.

Decoration models are uniquely suited to a correct modeling of chemical disorder (including vacancies) in a quasicrystal. Of course, a hyperspace fit to Bragg data can incorporate mixed occupation of a site type, but it is highly implausible (from the viewpoint of the structural energy) that the occupations of neighboring sites

¹ Keywords: A. quasicrystals, C. crystal structure and symmetry, C. scanning and transmission electron microscopy, D. crystal binding and equation of state

vary *independently* of each other. If the occupations are strongly correlated, then the mean structure may differ significantly from any particular real structure; this matters e.g. because the electronic structure is quite sensitive to the TM-TM contacts in $d(\text{AlNiCo})$ [12]. The tiling decoration is a very convenient way to account for such occupation correlations, by ascribing the randomness to the tiles and not the decoration. The ultimate criterion of a decorated model – fixing e.g. the appropriate size of tile – is that the ensemble of allowed tilings corresponds one-to-one with the ensemble of low-energy arrangements in an atomistic model.

A decoration description replaces the independent real coordinates of many atoms by tiling degrees of freedom, which are discrete and many times fewer. When the decoration is deterministic and disjoint (each atom bound to a particular tile or tile-related geometric object), then the atoms' interaction energies can be expressed as a function solely of the tile configuration, called the “tile Hamiltonian” $\mathcal{H}_{\text{tile}}$. This facilitates faster Monte Carlo simulations, on the comparatively few tile degrees of freedom, in order (i) to reveal supertilings in the process of discovering the atomic structure, as in this work; (ii) to predict diffuse scattering, or (iii) eventually to measure the phason elastic constants (which govern the diffuse wings surrounding Bragg peaks.) Armed with a reliable $\mathcal{H}_{\text{tile}}$, one can also simulate three-dimensional samples to obtain quantitative estimates of the perfection of the long-range order and the strength of diffuse diffraction.

This approach may also be the easiest way to resolve, for a particular stable quasicrystal, whether or not it is entropically stabilized. It is stabilized by energy favoring a quasiperiodic state if $\mathcal{H}_{\text{tile}}$ happens to implement the Penrose ‘matching rules’. That *almost* occurs in $d(\text{AlCuCo})$, as modeled with potentials like those used in the present work [13].

Our challenge, then, is to find the decoration rule and the tile-packing constraints without any bias, apart from the above-mentioned assumptions about the lattice constants. A caveat to keep in mind is that the results will probably be quite sensitive to the exact composition and number density.

III. INPUTS: POTENTIALS AND CONSTRAINTS

The main input to our calculations is a set of atom-atom pair potentials $V_{ij}(r)$ for species i and j , six distinct functions in the case of a ternary alloy. They are given by Moriarty’s “generalized pseudopotential theory” (GPT) [14–16], a systematic expansion of the total energy as a sum $E_0 + E_1 + E_2 + \dots$, where the E_n term depends on n atoms, but we use only the $n = 2$ terms. The first-neighbor well of the raw V_{TMTM} is unphysically deep (which would be canceled by E_3 in the systematic theory). Therefore our V_{TMTM} potentials were empirically modified, by fitting a short-range repulsive

correction so as to match all the forces in a full density-functional calculation on a small (50 atom) approximant of $d(\text{AlNiCo})$ [16]. There is strong support that our $V_{ij}(r)$ have the correct r dependence and relative strength, since they predict the Al-Co and Al-Ni phase diagrams pretty well [15] (as a function of concentration at $T = 0$); however the ternary Al-Ni-Co phase diagram was not attempted. On the basis of the simulated melting temperature and phonon spectra, we do suspect that our potentials are $\sim 30\%$ stronger than the reality.

Like the similar Al-TM potentials of Phillips, Zou, and Carlson, used earlier in Refs. [13] and [17], the GPT potentials depend implicitly on the net valence electron density, and exhibit strong “Friedel oscillations” as a function of distance (tails decaying as $\cos(2k_F r + \delta)/r^3$). For example, $V_{\text{AlTM}}(r)$ and $V_{\text{TMTM}}(r)$ show four prominent minima in the range $r \leq 8.5 \text{ \AA}$; such minima are quite important in deciding the structure [17,18].

Notice that $V_{\text{AlAl}}(r)$ is practically zero after its hard core radius $\sim 2.9 \text{ \AA}$: there is not even a nearest-neighbor well, just a shoulder on the tail of the hard-core. The V_{AlTM} potentials have very deep nearest-neighbor wells: this creates the illusion of a TM-TM repulsion, but really TM-TM neighbors are avoided mainly to make more room for Al in the TM coordination shells. However, at roughly 30% TM content, some TM-TM contacts are unavoidable; they are all Ni-Ni, since V_{AlCo} has a deeper well than V_{AlNi} . Finally, the V_{TMTM} potentials have their deepest well at second-neighbor ($\sim 4.2 \text{ \AA}$) distances. The consequence of all this is that the TM atoms form a rather rigid and somewhat uniformly spaced network [19], while Al atoms move rather freely to follow the potential wells or troughs created by the TM arrangement. (See Sec. V for more discussion).

Our use of these potentials imposes some limitations. We omitted the $n = 0$ term, which depends only on the valence electron density, and is the largest contribution to a metal’s total energy. Hence we can make valid comparisons only between structures with (practically) the same valence electron density. We cannot meaningfully predict the lattice constants. Nor can we even expect the quasicrystal phase to be globally stable according to our potentials, since they might spuriously favor phase-separation.

In view of the above-mentioned pitfalls for a brute-force approach, we adopted as a *second* input the experimental *lattice constants* [2]: the stacking period is $c = 4.08 \text{ \AA}$ and the quasilattice constant in the decagonal plane is $a_0 = 2.45 \text{ \AA}$. We only seek the lowest energy among arrangements on this framework. This highly constraining assumption still permits a vast ensemble of possible structures.

IV. METHODS AND RESULTS

Our methods are a mix of tile-flip Monte Carlo, atom-hopping Monte Carlo, relaxation of atomic positions, and molecular dynamics. Our procedure is first to discover the favorable low-energy motifs through Monte Carlo annealing, then to remove unnecessary degrees of freedom, and repeat, producing successively more constrained models. Having fewer degrees of freedom the latter are much faster to simulate at low temperatures. At the end, we can investigate the effects of letting atoms depart from ideal sites.

The initial stage of our exploration stacks two independent small (edge a_0) Penrose rhombic tilings, in a vertical space of one lattice constant $c = 4.08 \text{ \AA}$ and the only allowed atom sites are on vertices. A manageable size was 50 atoms on 72 candidate sites, initially on a good Penrose-tiling approximant; periodic boundary conditions are used in all directions (and at all stages of exploration). The atoms – initially chosen to approximate the experimental density and composition of the Ni-rich “Basic Ni” phase – hop as a lattice gas on these sites. This allows sufficient freedom for the atoms, if they “want”, to adopt any of the decagonal structure models – with stacking period $c = 4 \text{ \AA}$ – that were hypothesized at one time or another [20,21]. The Monte Carlo moves permit swaps of the species between two nearby sites (“vacant” is a special case of species!), as well as “tile flips” which reshuffle the three rhombi in a fat or thin hexagon in the same layer.

After this model is slowly cooled to zero temperature, if the initial composition was rightly chosen, one obtains a *one-layer* Hexagon-Boat-Star (HBS) tiling of edge length a_0 , with a *two-layer* decoration in which the allowed sites lie over vertices of the Penrose rhombi (into which HBS tiles may be decomposed) or an additional site in each Fat rhombus. This decoration places Al atoms over the HBS vertices (even and odd vertices alternate between even and odd layers). Isolated Co atoms sit over each Boat and Star tile center, ringed by possible Al sites; in the Star at most two Al can be present, out of five ideal sites in this ring. Particularly characteristic are the vertical zigzag chains, with Ni in each layer (appearing as NiNi pairs in Fig. 1), over the interior of every Hexagon tile. However, NiNi may be replaced by CoAl in some places. Decorating a tiling with the same H/B/S ratios as the quasiperiodic Penrose tiling yields an ideal composition $\text{Al}_{0.700}\text{Ni}_{0.207}\text{Co}_{0.093}$ and atomic volume 14.16 \AA^3 . This composition coincides with the experimental Basic Ni phase, but the number density of atoms is at least 5% greater than in experiment.

For the next stage of modeling, to discover larger-scale regularities, the small HBS tiles which emerged from the initial stage are elevated to fundamental objects, either with a rigid decoration or with some atoms fixed and others forming a lattice gas. The allowed tile flips are reshufflings of fat hexagons of the underlying rhombus

tiling, provided the result is a valid HBS tiling and conserves the atom content. Additionally the Al pair inside the Star tile can rotate among five allowed orientations. From this simulation, it emerges that the Hexagon tiles containing Ni chains only touch tip-to-tip, so that the angles relating them are multiples of 72° . In fact, (see Fig. 1) the long axes of the Hexagons form edges of an HBS *supertiling* with an inflated edge length $\tau^2 a_0$, where $\tau \equiv (1 + \sqrt{5})/2$.

V. THE 20 \AA DECAGON CLUSTER

We now compare our results with well-known structure models, organizing the discussion around the famous 20 \AA diameter decagon cluster, which is prominent in electron-microscope images and in most diffraction refinements as well. (The ideal decagon diameter is actually $2\tau^3 a_0$.) Such decagons indeed appear in our structures [22]; Fig. 1 is centered on one of them. Z-contrast images, in which the intensity is a direct projection of atoms weighted by squared atomic number, reveal the TM positions [6,7]; the TM (and most Al) positions proposed by Ref. [7] are practically the same as in our version of the cluster.

For a more detailed comparison, we focus on three recent structural studies [4–6]. All of these, *and our simulation*, agree on the following details of the projection: (1) the outer decagon (edge length $\tau^2 a_0$) has Al on each vertex and a pair of TM atoms on each edge, which we identify as Ni. (2) A middle decagon (edge τa_0) has TM atoms on each vertex, which we identify as Co. (3) An inner decagon (edge a_0) has Al on each vertex. (4) In the center, the 10-fold symmetry is broken and a sort of isosceles triangle is observed, with one TM (we say Co) at the unique corner and pairs of TM (we say NiNi) at the base corners. The cluster is evident in Ref. [4] on the right side of their Fig. 7, as a combination of a Boat tile + 2 Hexagon tiles, just as in our Fig. 1.

Detail (4) is somewhat controversial, since some decagon images have non-triangular centers. Indeed, the density maps from the refinement of Ref. [5] show *six* strongly TM sites at the center of many (but not all) of the 20 \AA decagons. We ascribe this to *stacking flips* between one layer and the next layer (see Sec. VI), seen in projection, as in the right-side decagon of Fig. 2.

The simulations we described up till now implicitly assumed a strict $c = 4.08 \text{ \AA}$ periodicity in the stacking direction, neglecting (like so much other modeling) the fact that decagonal quasicrystals are three-dimensional. To obtain the configuration in Fig. 2, we increased the periodicity to $2c$, i.e. two HBS layers, which initially were the same tiling. First a tile-flip was made in one of the two HBS layers, then the tilings were decorated, annealed by MD, and relaxed to an energy minimum.

In a fifth, controversial detail of the decagons, our model initially disagreed with experiments in which ev-

every edge of the middle decagon shows a *pair* of Al atoms. These sites form vertical zigzag chains, but they cannot all be occupied since they are separated by essentially the interlayer spacing $c/2 = 2.08 \text{ \AA}$. In our fixed-decoration model, then, these sites are occupied in only one atom layer, with separation c , so only one atom is visible on each edge. We found that, after molecular dynamics (MD) at 1000K followed by relaxation, some Al neighbors of the Co atoms shifted to the middle-decagon edges, which now present Al doublets in projection, in agreement with experiment.

To further understand what happens with these atoms, the time-average of the Al positions during the MD simulation is shown in Fig. 3. Some 40% of Al atoms are rather delocalized, and would need a highly anisotropic Debye-Waller factor in a crystallographic fit. [24] The vertical projection (Fig. 3(a)) shows, consistent with our remarks on the potentials (Sec. III), that each Co atom in the middle decagon is surrounded by a potential trough in which Al atoms appear almost free to roll like ballbearings [25].

A slice along a vertical plane further clarifies the Al behavior: a second type of trough extends vertically, with a zigzag shape, and in fact connects with the circular troughs. In our simulations with a cell $2c$ in the vertical direction, we found *three* Al atoms appearing in each zigzag trough (per $2c$, i.e. per 4 atom layers). Notice that the z displacement of two of these atoms makes the layer puckered, as is already known from diffraction [5], and implies a local cell-doubling along the c axis, similar to the $\text{Al}_{13}\text{Fe}_4$ or $\text{Al}_{13}\text{Co}_4$ decagonal approximants.

The symmetry-breaking of the cluster interior was recently predicted from energies by a full *ab-initio* calculation [26]. They find, from a quite different starting point than ours, the identical arrangement of the 5 Al + 5 TM atoms (per atomic bilayer) found at the cluster's center. However, they rejected the possibility of Al doublets on the middle decagon edges without trying z relaxations, nor did they address Co/Ni ordering. We find it striking that our mere pair potentials sufficed to obtain the experimentally indicated form of symmetry breaking in the cluster center, while using *no experimental input whatsoever* regarding the positioning of Al relative to TM atoms.

VI. TILE HAMILTONIAN AND THREE-DIMENSIONAL STACKING

To model a large, three-dimensional sample using a tile Hamiltonian, we cannot demand perfect periodicity in the z direction. (One reason is that the “entropic stabilization” explanation of quasicrystal order requires an extensive entropy.) So, we represent each bilayer of atoms by a distinct HBS tiling, and constrain adjacent tilings in the stack to differ by “stacking flips”, which are exactly the same reshufflings that constitute our Monte Carlo tile-flips.

We also found (from simulations) that – among (small) HBS tilings in which H tiles form a network touching tip-to-tip – the in-plane tile Hamiltonian is dominated by interactions between “H(NiNi)” tiles (Hexagon tiles decorated by NiNi). Thus we suggest

$$\mathcal{H}_{\text{tile}} = c_{72}N_{72} + E_{\text{sf}}N_{\text{sf}}. \quad (1)$$

where N_{72} is the number of H(NiNi) tile pairs related by a 72° rotation about their common tip, and N_{sf} is the total number of stacking flips.

We fitted $c_{72} = 0.218 \text{ eV}$ [1] from the simulation with ideal sites; this is positive since the 72° relation of H(NiNi) tiles creates intertile NiNi neighbors, and thus reduces the number of (favorable) AlNi pairs. The structure minimizes N_{72} by arranging that in some places, an H(NiNi) tile has one tip which contacts no other H(NiNi), and sees CoAl (at a 144° angle) in place of NiNi. That may be accomplished in two ways. If we re-allow lattice-gas hopping on the *interior* sites of the (small) HBS tiles, and properly adjust the stoichiometry [1], we obtain the same old rigid decoration, except that a few H(CoAl) tiles appear, as illustrated in Fig. 1. On the other hand, if we retain the rigid NiNi decoration of small H tiles, the CoAl belongs to the interior of a Boat tile, and the large HBS tiling acquires a fourth kind of tile (“Bowtie”), as in Fig. 4(a) of Ref. [1].

Existing experiments can in principle measure E_{sf} . The time-dependent local “phason” flips [27], observed at $T \approx 1200 \text{ K}$ by TEM through very thin samples of $d(\text{AlCuCo})$, can only occur by nucleating a “stacking flip” at one surface, which subsequently random-walks to the other surface. Video images [27] display an intermediate state for a noticeable fraction – say 10% – of the time, so that with a sample thickness estimated at 100 \AA (25 bilayers), one would very roughly estimate $E_{\text{sf}} \approx 0.3 \text{ eV}$ in $d(\text{AlCuCo})$. It would be exciting if such observations could be analyzed quantitatively. In our simulation, with rigid atoms decorating ideal sites, $E_{\text{sf}} \approx 1.4 \text{ eV}$. However, relaxation (as in Fig. 2) nearly cancels this energy cost, indeed $E_{\text{sf}} \approx -0.2 \text{ eV}$ in very preliminary results, which should not be compared with the experiments on a different quasicrystal. (Physically, $E_{\text{sf}} < 0$ probably implies a period $2c \approx 8 \text{ \AA}$ modulation.)

VII. DISCUSSION

We find it remarkable that, with quite sketchy experimental input, our simulations appear competitive with single-crystal diffraction as a way of discovering this rather complex structure. This occurs despite the shortcomings of the pair potentials – our omission of 3-body terms, and the likelihood that the V_{AlTM} we use is stronger than the real one. Even if the connection to the microscopics is not quantitative, one may still obtain the large-scale order quite well: that depends mostly on

the tile Hamiltonian (1) having the proper form, which is more robust than the numerical values of the coefficients.

It should also be pointed out that even imperfect potentials could be quite useful for *augmenting* a fit of diffraction data. A combination of energy and diffraction data could overcome minor spurious features in refinements [23].

Our results strongly suggest that, in *this* alloy system, stability of the quasicrystal requires a ternary not only to tune the electron density, as in the Hume-Rothery picture, but also because each species fills a particular type of site. Thus it would be highly desirable to explore some other composition regimes in simulations. The Co-rich “basic Co” subphase of $d(\text{AlNiCo})$ would be of particular interest. It exhibits much stronger diffuse scattering than Basic Ni, particularly halfway between the layers of Bragg peaks in reciprocal space, indicating a local tendency to doubling the c periodicity (8 Å structures).

Our constraint that the atoms sit on ideal sites in the initial stage of energy optimization has considerable potential to distort the conclusions. Clearly, atom displacements have a very strong effect so it is crucial to include these for a final answer. Small adjustments of position can gain as much energy as swaps of species, and in some cases the optimal sites may lie halfway between ideal sites, or between ideal layers – the so-called “puckered” layers. We do allow such relaxations in later stages, after determining a decoration, but it appears possible that a different decoration would be obtained, if we allowed relaxations in the early stages. This seems to be the most serious drawback of the lattice-gas approach [13] we used. Its advantages are that the systematic Monte Carlo exploration is not biased by its users’ prejudices, and furthermore it could readily be adapted to $T > 0$ (the temperatures at which the quasicrystal phase is stable). Nonzero temperature probably affects the result just as strongly as relaxed positions do.

Within the framework of pair potentials and tile-decoration representation of the structure, a different approach is possible [17], whereby relaxed sites are used in the main discovery process. To implement this so that only valid tile decorations get explored, one performs relaxations with the decoration-equivalent atoms of a given class (“orbit”) being constrained to move together. However, that method is ad-hoc, depending on its users’ educated guesses as to the tilings and decorations to be tried. Future work should strive to blend the best features of these two approaches to using decorations with potentials for the discovery of structures.

This research was supported by the Department of Energy grant DE-FG02-89ER-45405 and by National Science Foundation grant DMR-0111198. We thank E. Cockayne, F. Gähler, E. Abe, and K. Edagawa for discussions.

- [1] M. Mihalkovič, I. Al-Lehyani, E. Cockayne, C. L. Henley, N. Moghadam, J. A. Moriarty, Y. Wang, and M. Widom, “Total-energy-based prediction of a quasicrystal structure”, to appear, *Phys. Rev. B*; see www.arXiv.org, cond-mat/0102085.
- [2] S. Ritsch, C. Beeli, H. U. Nissen, T. Gödecke, M. Scheffer, and R. Lück, *Phil. Mag. Lett.*, 74, (1996) 99-106; A. P. Tsai, A. Fujiwara, A. Inoue, and T. Masumoto, *Phil. Mag. Lett.*, 74 (1996) 233-40.
- [3] S. Ritsch, C. Beeli, H. U. Nissen, T. Gödecke, M. Scheffer, and R. Lück, *Phil. Mag. Lett.* 78 (1998) 67-76.
- [4] H. Takakura, A. Yamamoto, and A.-P. Tsai, *Acta Cryst. A* 57 (2001) 576-585.
- [5] A. Cervellino, T. Haibach, and W. Steurer, submitted to *Acta Cryst. B*, 2001.
- [6] Y. Yan, S. J. Pennycook, and A. P. Tsai, *Phys. Rev. Lett.* 81 (1998) 5145-8.
- [7] E. Abe, K. Saitoh, H. Takakura, A. P. Tsai, P. J. Steinhardt, and H.-C. Jeong, *Phys. Rev. Lett.* 84 (2000) 4609-12.
- [8] Our Ni/Co assignments (based on potentials) are completely different from those of Ref. [7], which were guessed so as to match the site frequencies in a simple, disorder-free decoration with the experimental stoichiometry.
- [9] F. Lançon, L. Billard, and P. Chaudhari, *Europhys. Lett.* 2, (1986) 625; M. Widom, K. J. Strandburg and R. H. Swendsen, *Phys. Rev. Lett.* 58 (1987) 706.
- [10] M. Dzugutov, *Phys. Rev. Lett.* 70 (1993) 2924.
- [11] J. Roth and A. R. Denton, *Phys. Rev. E* 61 (2000) 6845-6857.
- [12] M. Krajčí, J. Hafner, and M. Mihalkovič, *Phys. Rev. B* 62 (2000) 243-55. The structure models used disagree with our present model in some important points.
- [13] E. Cockayne, and M. Widom, *Phys. Rev. Lett.* 81 (1998) 598-601.
- [14] J. A. Moriarty, and M. Widom, *Phys. Rev. B* 56 (1997) 7905-17.
- [15] M. Widom and J. A. Moriarty, *Phys. Rev. B* 58 (1998) 8967-8979.
- [16] I. Al-Lehyani, M. Widom, Y. Wang, N. Moghadam, G. M. Stocks, and J. A. Moriarty, *Phys. Rev. B* 64 (2001) 075109.
- [17] M. Mihalkovič, W.-J. Zhu, C. L. Henley, and R. Phillips, *Phys. Rev. B* 53 (1996) 9021-45.
- [18] Stabilization due to Friedel oscillations is *mathematically equivalent* to the Hume-Rothery stabilization mechanism (if energies are computed in second-order perturbation theory); the difference is that one is expressed in real space and the other in reciprocal space.
- [19] This rationale for structural tendencies emphasizes second-neighbor TM-TM interactions, whereas Ref. [1] emphasized first-neighbor Al-Al and Al-TM interactions with Al atoms at ideal sites. Perhaps the best ternary structures evade “frustration”, by being independently optimal for *both* TM-TM and Al-related potentials.
- [20] C. L. Henley, *J. Non-Cryst. Solids* 153&154 (1993) 172-176.
- [21] In particular, a similar lattice-gas annealing using potentials representing $d(\text{AlCuCo})$ obtained a somewhat different atomic structure. (Ref. [13].) In contrast to the

present formulation, the lattice-gas sites of Ref. [13] lay on a fixed quasilattice. The quasilattice sites must be more densely placed in order to obtain comparable results without the freedom of tile flips.

[22] The 20 Å rings are commoner in images than in our simulations of single bilayers. One possible explanation is “stacking flips” between the layers. This was illustrated in Fig. 8 of Ref. [23], using the same d (AlNiCo) structure reported in the present paper. Just a couple stacking flips, seen in projection, create an apparent decagon, and they also tend to symmetrize the appearance of the decagon interior.

[23] C. L. Henley, V. Elser, and M. Mihalkovič, *Z. Kristallogr.* 215 (2000) 553-568.

[24] Recent experiments which extract differences in the TEM images of Basic Ni d (AlNiCo) samples upon rapid temperature changes, indicate smearing of probability density for the five Al atoms at the decagon center, which is reminiscent the distributions in our Fig. 3. (E. Abe and A. P. Tsai, this conference.)

[25] Independent MD simulations, using our structure and potentials (Refs. [14-16]), suggest that Al atoms can cyclically permute in troughs around a Co atom or around the entire decagon. (Franz Gähler, personal communication).

[26] Y. Yan and S. J. Pennycook, *Phys. Rev. Lett.* 86 (2001) 1542-1545.

[27] K. Edagawa, K. Suzuki, and S. Takeuchi, *Phys. Rev. Lett.* 85 (2000) 1674, and this conference.

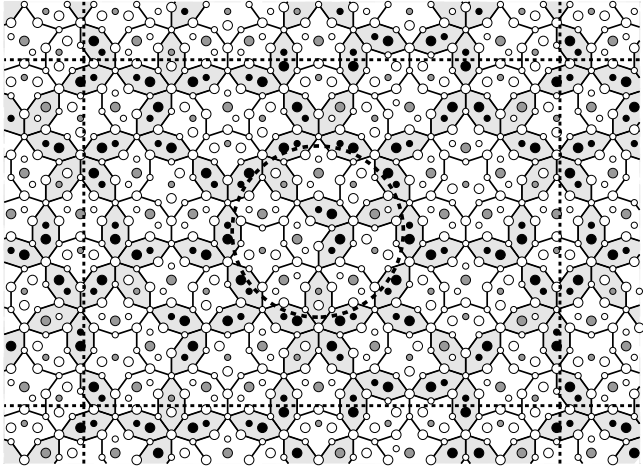


FIG. 1. Lowest-energy configuration obtained from a simulation with variable occupancy interiors. Circles are colored with the following convention: empty=Al, gray=Co, black=Ni; the size of the symbol represents the z coordinate. Shaded small hexagon tiles, occupied by either NiNi pairs or AlCo pairs, form the edges of an HBS supertiling. Dashed circle indicates a 20 Å decagon cluster. This is the same configuration as Fig. 4(b) of Ref. [1].

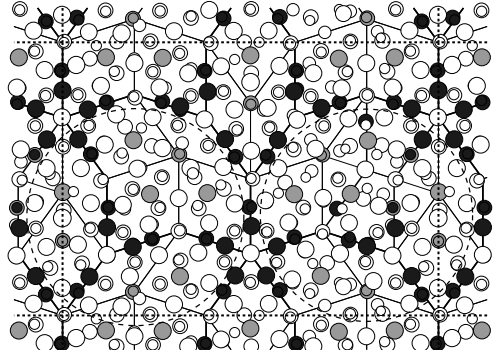


FIG. 2. Two bilayers (thickness $2c$), with periodic boundary conditions in all directions, after a tile flip in one bilayer, followed by molecular dynamics and relaxation to an energy minimum. Black lines are HBS supertile edges (length $\tau^2 a_0$). The dashed circles are imperfect 20 Å decagons – this cell is too small to contain complete ones.

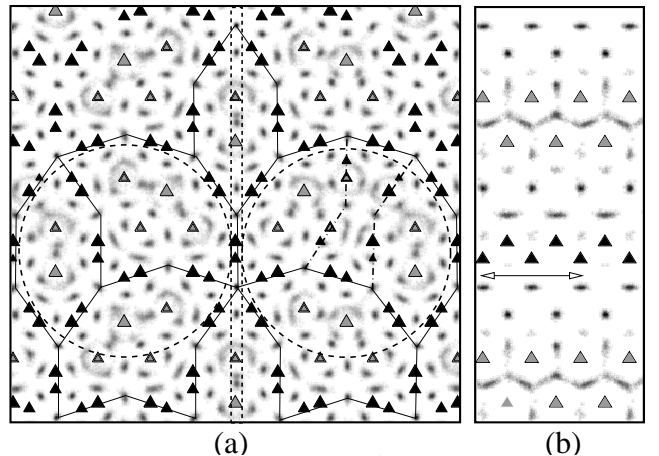


FIG. 3. Probability density of Al atom centers during a molecular dynamics simulation of the same configuration as in Fig. 2. TM locations are indicated by triangles, with the same coloring and size conventions as the previous figures. Edges of the large HBS tiles are marked by lines. (a) Projection onto xy plane. (b) Projection onto the yz plane of the narrow slab outlined by a dashed rectangle in (a). The pattern repeats with the z period 8 Å. (Note this slice actually cuts through an H tile but not a 20 Å cluster.)